Experimental investigation of the flow-induced vibration of hydrofoils in cavitating flows

Guoyu Wang, Qin Wu, Biao Huang[1], Yuan Gao
Beijing Institute of Technology, 5 South Zhongguancun Street, Beijing 100081, China

E-mail: huangbiao@bit.edu.cn

Abstract. The objective of this paper is to investigate the correlation between fluid induced vibration and unsteady cavitation behaviours. Experimental results are presented for a modified NACA66 hydrofoil, which is fixed at α=8°. The high-speed camera is synchronized with a single point Laser Doppler Vibrometer to analyze the transient cavitating flow structures and the corresponding structural vibration characteristics. The results showed that, with the decreasing of the cavitation number, the cavitating flows in a water tunnel display several types of cavitation patterns, such as incipient cavitation, sheet cavitation and cloud cavitation. The cavity shedding frequency reduces with the decrease of the cavitation number. As for the cloud cavitation regime, the trend of the vibration velocity goes up with the growth of the attached cavity, accompanied with small amplitude fluctuations. Then the collapse and shedding of the large-scale cloud cavities leads to substantial increase of the vibration velocity fluctuations.

1. Introduction

Flow induced vibration is one of the major issues in a wide range of fields, such as fluid mechanics, structural mechanics, computational fluid dynamics and acoustics. Discussions about these subjects can be found in the references [1-4]. Yao et al. [5] experimentally investigated the flow induced vibration on a hydrofoil with Donaldson trailing edge shape. The results showed that the hydrodynamic damping is significantly increased with the Donaldson cut and the vibration is significantly reduced with a slight modification of the trailing edge without alternation of the hydrodynamic performances. Ducoin et al. [6] experimentally characterized that the vibrations of hydrofoil were induced by the laminar to turbulent boundary layer transition and depended on the vortex shedding frequency.

Since the cavitation involves complex interaction between phase-change and vortex structures, the unsteady breakdown and shedding of the cavities will induce strong transient loads and lead to further hydrodynamic instabilities, even structure failures. Hence, the flow induced vibration under cavitating flows has attracted considerable interests. Torre [7] conducted a series of experiments to investigate the influence of the sheet cavitation and supercavitation on the added mass effects experienced by a modified NACA0009 hydrofoil. The results showed that the added mass decreases when cavitation appears because of the increased cavity length. Amromin and Kovinskaya [8] analyzed the vibration of an elastic hydrofoil with an attached cavity in periodically perturbed flow, where a beam equation was used to describe the hydrofoil vibration. The results showed that the structural vibration increased significantly due to the cavitation. The high-frequency band was attributed to the hydrofoil resonance

[1] To whom any correspondence should be addressed.

with the cavity adding a certain damping and the low-frequency band was corresponding to the cavity volume fluctuations.

Although the phenomenon of flow induced vibration has been widely investigated, the correlation between fluid induced vibration and unsteady cavitation behaviours are still not obvious, since it's difficult to measure the unsteady structural vibration and moreover synchronize the observation of cavitation behaviours with the measurement of vibration fluctuations. The objective of this work is to shed light on the unsteady cavitating flow and corresponding vibration characteristics, and to offer a basis for future numerical validation studies.

2. Experimental set-up

Experimental studies are conducted in a closed-loop cavitation tunnel at Beijing Institute of Technology [9], which is shown in figure 1. The test section is 0.7m long and has a rectangular section with width of 0.07m and height of 0.19m. As shown in figure 2, the modified-NACA66 [10] is placed with α=8°, which is subjected to a nominal free stream velocity of U_∞=8m/s, yielding a moderate Reynolds number of $Re=U_\infty c/\nu=6.0\times10^5$. The outlet pressure is set to vary according to the cavitation number $\sigma=(p_\infty-p_v)/(0.5\rho_l U_\infty^2)$. It should be noted that a small gap (1mm) is existed between the front wall of the test section and the free end of the hydrofoil, so that the tip section is free to enable the vibration of the hydrofoil.

The cavitation patterns are observed with a high-speed digital camera (HG-LE, by Redlake) [10] and 2500 fps is used in this study. The vibration velocities are measured on the pressure side of the hydrofoil with a single point Laser Doppler Vibrometer (LDV) Polytec PSV-100 [10]. The smallest possible measurement range (20mm/s as its peak) is used to optimize the signal-to-noise ratio and the sample frequency is 22kHz, with the measure point located at the x/c=0.2 in the mid-plane of the hydrofoil. Then the velocity signal can be fed into digital inputs of a data acquisition system [9].

Figure 3 shows the layout of simultaneous sampling system, the high-speed visualization and unsteady vibration measurement setups are combined by a controller. When the controller is triggered, the cavitation images and unsteady vibration velocities will be captured simultaneously. Even though the sampling rate of high-speed camera is far less than that of LDV system, each cavity image has its own corresponding value of the vibration velocity according to the actual time. The uncertainty of simultaneous sampling is negligible compared with periodic time of the unsteady cloud cavitation [9].

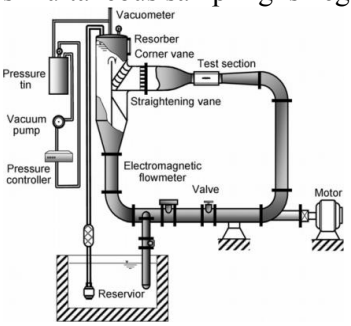

Figure 1 Schematic of the cavitation tunnel

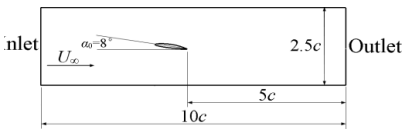

Figure 2 Sketch of the foil's position in the test section

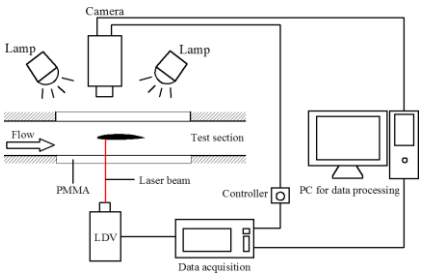

Figure 3 Layout of simultaneous sampling system

3. Results and discussion

3.1. The spectral analysis of the vibration velocities in different cavitation regimes

Figure 4 shows the time evolution of the typical cavity shapes observed in the experimental visualization for different cavitation regimes with σ=2.3, 1.9, 1.2 and 0.8. It is shown that the cavitation inception is observed at about σ=1.9. In this regime, the cavitating flow appears in white at the leading edge of the foil, indicating that it contains large number of micro-sized vapor bubbles. Reducing the cavitation number, the cavitation changes from the incipient cavity to sheet cavity at about σ=1.2. Although the cavity is attached at the leading edge of the foil, the rear portion of the

sheet cavity is unsteady and rolls into small bubbly vortices that shed intermittently. Further lowing the cavitation number to about σ=0.80, the sheet cavity grows and the trailing edge becomes increasingly unsteady accompanied with cloud cavities shedding massively.

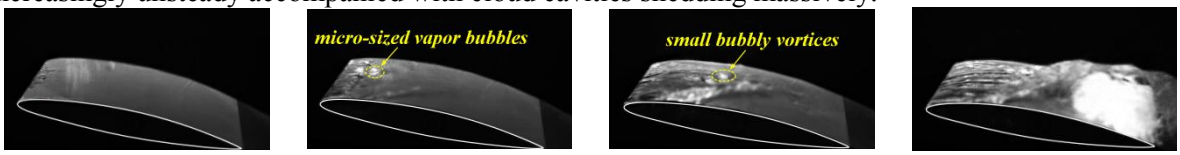

σ=2.3 σ=1.9 σ=1.2 σ=0.8

Figure 4 The typical cavitation patterns for different cavitation number

To investigate the effects of cavitation on hydroelastic response, figure 5 shows spectral characteristics of the measured vibration velocity of the hydrofoil, which are obtained by the Fast Fourier Transform of the vibration velocity. One of the main flow-induced frequencies, as shown in the amplitude peaks in figure 5, are 165Hz, 90Hz and 18Hz for the cases with σ=1.9, 1.2 and 0.8 respectively, are accordance with the cavity shedding frequency. This is confirmed by comparing the spectra to the cases of fully turbulent flow, where such components are not visible. The cavity shedding frequency decreases with the decrease of the cavitation number because the cavity increases in length and requires more time to evolve between the subsequent cavitational cycles.

The Strouhal number $Str=fc/U$ against $\sigma/2\alpha$ is plotted in figure 6. Reasonable agreement can be obtained between the present results and pervious experimental measurements [11-13] for different hydrofoils. Although some discrepancies exited between the foils at a constant value of $\sigma/2\alpha$, all cases show similar trends. The Strouhal number Str remains almost constant when the values of $\sigma/2\alpha$ less than approximately 4, and increases with $\sigma/2\alpha$ for larger $\sigma/2\alpha$ values.

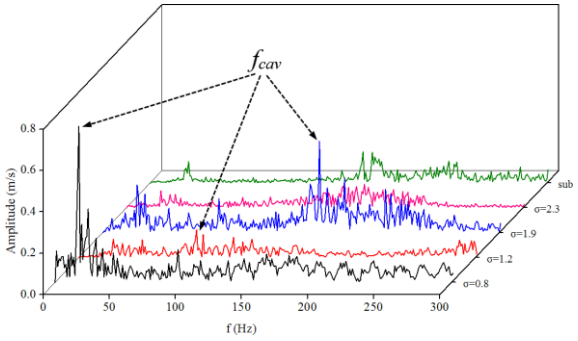

Figure 5 The effect of σ on the frequency spectrum of vibration velocity

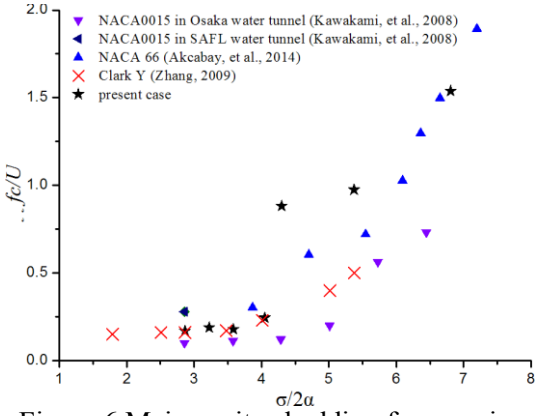

Figure 6 Main cavity shedding frequencies compared with results in Refs.

3.2. The vibration velocity associated with the unsteady cloud cavitation behaviors

As to the regime of cloud cavitation, the unsteady breakdown and shedding of the cavity occurs violently, which leads to highly unsteady hydrodynamic forces on the hydrofoil, and hence may result to strong dynamic instabilities [14-15]. In the present study, when the cavitation number reduces to σ=0.8, the transient cloud cavitation develops, which has a distinctly quasi-periodic pattern. Figure 7 shows the time evolution of the vibration velocity within several cycles, followed by the experimental observation of the cavity shapes at representative times in one cycle, as shown in figure 8. The period of the cloud cavitation T_{cycle} is about 55ms, which is corresponding to $5.8c/U_\infty$. Combined figures 7 and 8, the evolution of the transient cavity shapes and the corresponding vibration characteristics could be divided into two stages: (I) development of the attached cavity (from t_1 to t_3) and (II) shedding and collapse of the attached cavity (from t_3 to t_{12}). The principal characteristics is that the trend of the vibration velocity goes up with the growth of the attached cavity (seen the red dash line shown in figure 7), accompanied with small amplitude fluctuations. Then the vibration velocity tends to decrease with large amplitude fluctuations, which is corresponding to the shedding and collapse of

the cloud cavity. The detailed development of the flow structures in this stage can be characterized as follows: From t_4 and t_6, the re-entrant jet begins to form at the rear part of the cavity, leading to the formation of the cloud cavity. As seen in figures 7 and 8(f), the moment (t_6) the cloud cavity breaks up from the primary attached cavity, the vibration velocity of the hydrofoil hits the peak. After that, from t_7 and t_{10}, the collapse of the large-scale cloud cavity leads to the substantial increase of vibration velocity fluctuations, as shown in figure 7, because the propagated pressure pulse and the energy released by the cavity collapse aggravate the vibration of the foil. This is also confirmed by Chen et al [9]. Finally, due to the unsteady shedding of the cavity, the amplitude of the vibration velocity fluctuations decrease.

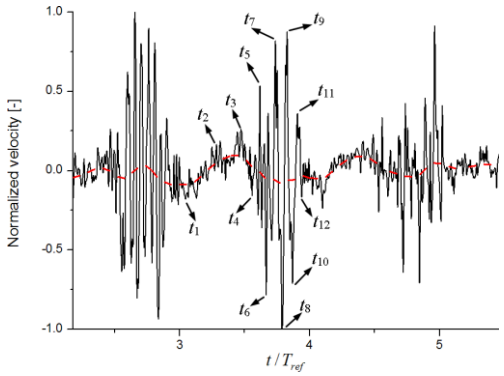

Figure 7 Time evolution of the vibration velocity.

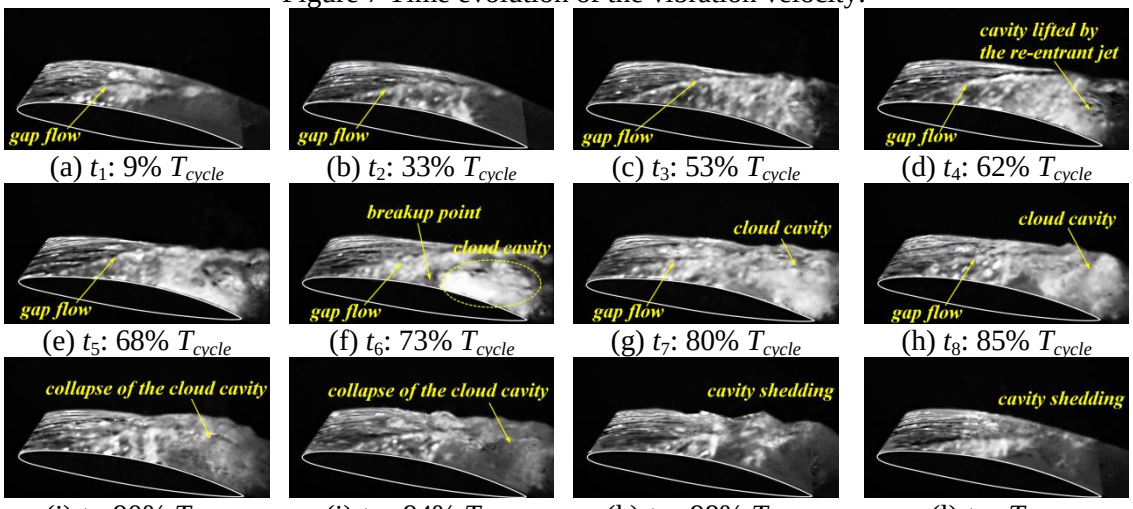

(a) t_1: 9% T_{cycle} (b) t_2: 33% T_{cycle} (c) t_3: 53% T_{cycle} (d) t_4: 62% T_{cycle}

(e) t_5: 68% T_{cycle} (f) t_6: 73% T_{cycle} (g) t_7: 80% T_{cycle} (h) t_8: 85% T_{cycle}

(i) t_9: 90% T_{cycle} (j) t_{10}: 94% T_{cycle} (k) t_{11}: 98% T_{cycle} (l) t_{12}: T_{cycle}

Figure 8 Time evolution of the cloud cavitation patterns.

4. Conclusions

In this paper, experimental studies are presented for a NACA66 hydrofoil with the angle of attack α=8° at Re=600,000 for different cavitation regimes (σ=2.3, 1.9, 1.2 and 0.8). The primary findings include:

(1) With the decreasing of the cavitation number, the cavitating flows in a water tunnel display several types of cavitation patterns, such as incipient cavitation, sheet cavitation and cloud cavitation. The cavity shedding frequency reduces with the decrease of the cavitation number because the cavity increases in length and requires more time to evolve between the subsequent cavitational cycles. And the vortex shedding frequency remains almost constant.

(2) For the cloud cavitation regime, the evolution of the transient cavity shapes and the corresponding vibration characteristics could be divided into two stages: (I) development of the attached cavity and (II) shedding and collapse of the attached cavity. During the first stage, the trend of the vibration velocity goes up with the growth of the attached cavity, accompanied with small

amplitude fluctuations. During the latter stage, the vibration velocity tends to decrease with large amplitude fluctuations, which is corresponding to the shedding and collapse of the cloud cavity.

(3) As for the correlation between fluid induced vibration and unsteady cavitation behaviours, the moment the cloud cavity breaks up from the primary attached cavity, the vibration velocity of the hydrofoil hits the peak. The collapse of the large-scale cloud cavity leads to the substantial increase of vibration velocity fluctuations, because the propagated pressure pulse and the energy released by the cavity collapse aggravate the vibration of the foil. Due to the unsteady shedding of the cavity, the magnitude of the vibration velocity fluctuation decreases.

Acknowledgements

This work was supported by the National Science Foundation of China (Grant No.51306020) and the Beijing Natural Science Foundation (Grant No.3144034).

References

[1] Ausoni P, Farhat M, Escaler X, Egusquiza E and Avellan F 2007 *ASME J. Fluids Eng.* **129** 966-73.
[2] Donaldson M E 1956 *J. Eng. Power* **78** 1141-47.
[3] Howe M S 1988 *J. Sound Vibration* **126**(3) 503-23.
[4] Seo J H and Lele S K 2009 *Proc. 7th Int. Symp. Cav.* Ann Arbor, Michigan, USA.
[5] Yao Z F, Wang F J, Dreyer M and Farhat M 2014 *J. Fluids Struct*. **51** 189-98.
[6] Ducoin A, Astolfi J A and Gobert M-L 2012 *J. Fluids Struct*. **32** 37-51.
[7] Torre D L, Escaler X, Egusquiza E and Farhat M 2013 *J. Fluids Struct*. **39** 173-87.
[8] Amromin E and Kovinskaya S 2000 *J. Fluids Struct*. **14**(5) 735-51.
[9] Chen G H, Wang G Y, Hu C L, Huang B and Zhang M D 2015 *Exp. Fluids* **56**(32) 1-11.
[10] Wu Q, Huang B, Wang G Y and Gao Y 2015 *Int. J. Multi. Flow* doi: http://dx.doi.org/10.1016/j.ijmultiphaseflow. 2015.03.023
[11] Akcabay D T, Chae E J, Young Y L, Ducoin A and Astolfi J A 2014 *J. Fluids Struct*. **49** 463-84.
[12] Zhang B 2009 Thesis of PhD, Beijing Institute of Technology.
[13] Kawakami D T, Fuji A, Tsujimoto Y and Arndt R E A 2008 *ASME J. Fluids Eng.* **130** 1-8.
[14] Arndt R E A 1981 *Ann. Rev. Fluid Mech.* **13** 273-328.
[15] Luo X and Ji B. 2012 *ASME J. Fluids Eng.* **134** 041202 1-10.